Journal of Colloid and Interface Science 351 (2010) 108–115

Contents lists available at ScienceDirect

Journal of Colloid and Interface Science

www.elsevier.com/locate/jcis

Sodium montmorillonite silylation: Unexpected effect of the aminosilane chain length

Filomena Piscitelli [a,b,*], Paola Posocco [c], Radovan Toth [c], Maurizio Fermeglia [c], Sabrina Pricl [c], Giuseppe Mensitieri [a], Marino Lavorgna [b,d]

[a] Department of Materials Engineering and Production, University of Naples Federico II, Piazzale Tecchio 80, 80125 Naples, Italy
[b] National Research Council, Institute for Composite and Biomedical Materials, Piazzale E. Fermi, 1, 80155 Portici, Naples, Italy
[c] Molecular Simulation (MOSE) Engineering Laboratory, DMRN, University of Trieste, Piazzale Europa 1, 34127 Trieste, Italy
[d] IMAST Technological District on Polymeric and Composite Materials Engineering and Structures, Piazzale E. Fermi 1, 80155 Portici, Naples, Italy

ARTICLE INFO

Article history:
Received 25 May 2010
Accepted 24 July 2010
Available online 1 August 2010

Keywords:
Organosilane
Na-MMT silylation
Molecular dynamics simulations

ABSTRACT

In this work, the silylation of sodium montmorillonite (Na-MMT) was performed in glycerol using 3-aminopropyltriethoxysilane, N-(2-aminoethyl)-3-aminopropyltrimethoxysilane and 3-[2-(2-aminoethylamino)ethylamino]-propyl-trimethoxysilane. The effects on the *d*-spacing of sodium montmorillonite (Na-MMT) upon reaction with three aminosilanes of different chain length were studied in details by combining experimental and computational techniques. Infrared spectroscopy was used to monitor the grafting process, while the degree of grafting was calculated using thermogravimetric analysis. X-ray diffraction experiments were carried out to evaluate the shift of the (0 0 1) basal spacing. It was found that the degree of silylation of Na-MMT increases with increasing the length of the aminosilane organic moieties, the overall aminosilane concentration, and temperature. The same beneficial effects were observed on the silicate *d*-spacing, as its value increases with increasing silane concentration and reaction temperature. Remarkably, however, increasing the length of the organic chains in the silane modifiers resulted in decreasing values of the Na-MMT interlayer distance. A rationale for this behavior is proposed on the basis of atomistic molecular dynamics simulation evidences.

1. Introduction

Because of their unique structure, layered silicates are largely employed in the production of polymer nanocomposites with improved physical properties with respect to the pristine polymeric matrix [1–3]. Enhanced mechanical-, thermal- and gas-barrier properties can indeed be achieved by adding small amounts of clay (<5% by weight) to a given polymer, and this in fact opens new avenues in the design and synthesis of a plethora of new, high-performance materials for which an array of advance applications can easily be envisaged. Montmorillonite (MMT) is one of the layered silicates currently most widely employed in the production of polymer–clay nanocomposites [1–3]. The crystalline structure of MMT is based on a regular arrangement of silicon tetrahedra (SiO_4^{4-}) and aluminum octahedra ($Al(OH)_6^{3-}$), the unit cell containing two tetrahedral and one octahedral layers. MMT layer has permanent negative charge on the surface of its layers because of isomorphous substitutions of Mg^{2+} for Al^{3+} or, rarely, Al^{3+} for Si^{4+} [3]. These negative charges are counterbalanced by the presence of first-group cations such as sodium or potassium, which locate in the proximity of the clay platelets within the gallery space [1]. The presence of these net charges then confers to the pristine structure of, i.e., sodium MMT (Na-MMT) a highly polar nature, and this, in turn, renders this silicate quite incompatible with the vast majority of organic polymers [2,3]. Accordingly, a simple dispersion of Na-MMT in a polymeric matrix will not produce a composite with improved properties compared to the neat macromolecule, because of the poor interfacial interactions between the Na-MMT hydrophilic reaction sites and the highly hydrophobic polymeric chains. Therefore, chemical modification of internal and external Na-MMT platelets plays a crucial role in polymer/clay nanocomposite formation. Several efforts have been done in order to reduce the hydrophilicity of the Na-MMT internal platelets; in particular the cation exchange reaction with a quaternary ammonium salt (see for example the case of Cloisite 30B) represents the most commonly used method to modify clay surface. This modification increases the interlayer spacing and creates a more favorable organophilic environment. However, the thermal instability of conventional ammonium ion-modified clay is a strong limitation for melt-compounding of polymer/organoclay composites. In fact, most of the

* Corresponding author at: Department of Materials Engineering and Production, University of Naples Federico II, Piazzale Tecchio 80, 80125 Naples, Italy. Fax: +39 (0) 81 775 88 50.
E-mail address: Filomena.Piscitelli@imcb.cnr.it (F. Piscitelli).

0021-9797/$ - see front matter © 2010 Elsevier Inc. All rights reserved.
doi:10.1016/j.jcis.2010.07.059

alkyl ammonium surfactants are known to undergo a degradation process at temperature at which the plastics are commonly processed [4]. For this reason, the silylation approach involving direct grafting reaction by using a coupling agent has recently attracted much attention, and represents a viable method to make compatible inorganic platelets and organic matrix [5–10]. The presence of broken bonds on the platelet edges are common for layered silicates, and leads to the formation of hydroxyl groups, which can be utilized for chemical modification by silylation reaction. By using an organosilane, it is then possible to covalently bond the organic functional groups onto the layer surface. Importantly, the functionalization of clay minerals with organosilanes can take place at three different sites: at the interlayer space, at the external surface and at the edges [11,12].

In terms of performances of silane-modified MMT nanocomposites, Zhao et al. [13] found that the use of chlorosilane-modified clay allowed the improvement of the mechanical behavior of polyethylene (PE)-based nanocomposites determining an increase of both glass transition temperature and elastic modulus in the glassy region. In particular, after trimethylchlorosilane (TMSCl) modification, the OH groups at the edge of clay platelets were reacted and the wetting ability between PE and organoclay was subsequently improved. Moreover, the loss of hydroxyl groups resulted in a decrease of cation exchange capacity (CEC), which caused a reduction in the strength of interaction between the platelets. Both these effects favorably concurred to improve the intercalation of PE into interlayers.

So far the silylation reaction has been widely performed using (3-aminopropyl)trimethoxysilane (A1100), TMSCl and glycidyl-propyl-triethoxysilane (GPTS) [12] as coupling agents. Among several investigations, it is here mentioned the work of Wang et al. [14], which found that Na-MMT modified by a small amount of A1100 as coupling agent is able to promote a high extent of exfoliation for epoxy/clay nanocomposites. However, to the best of our knowledge, the effects of other aminosilanes on the MMT final basal spacing have not been evaluated yet.

Accordingly, in this paper the silylation reaction of Na-MMT with three aminosilanes, each bearing three functional groups but characterized by different lengths of the alkyl chains, has been studied. The functionalized clay has been characterized by Fourier transform infrared spectroscopy (FT-IR), thermogravimetric analysis (TGA) and X-ray diffraction. In order to understand the effect of reaction conditions (e.g., reaction temperature and aminosilane concentration), two different routes were followed in performing the Na-MMT silylation reaction by using the A1100 as a proof-of-concept. The results obtained in terms of modified Na-MMT *d*-spacing were correlated with the corresponding values predicted from atomistic molecular dynamics simulations, and a molecular rationale for these experimental evidences has been formulated on the basis of the molecular modeling results.

2. Experimental

2.1. Materials

Sodium montmorillonite (Na-MMT) with cationic exchange capacity (CEC) of 92 mequiv/100 g was purchased from Southern Clay Products Inc., USA. Prior to its use, the Na-MMT was dried over night at 90 °C in *vacuum* conditions. 3-aminopropyltriethoxysilane (A1100), N-(2-aminoethyl)-3-aminopropyltrimethoxysilane (A1120), and 3-[2-(2-aminoethylamino)ethylamino]-propyl-trimethoxysilane (A1130) were obtained from GE Advanced Materials. All trifunctional silylating agents had a purity of 98%. Glycerol was purchased from Fluka. All chemicals were used as received.

2.2. Silylation reaction

To perform the silylation reaction of Na-MMT by aminosilanes, two different reaction conditions were used, in which both the reaction temperature and the amount of the aminosilane were varied, respectively. These two experimental routes, referred to, in the following as *Procedure 1* and *Procedure 2*, are summarized in Table 1.

Dried Na-MMT (1 or 5 g) were added to 100 ml of glycerol, and the resulting suspension was stirred at 60 °C for 30 min in nitrogen atmosphere. The same procedure was used to dissolve the aminosilane in glycerol. In this work glycerol was selected as the solvent, since, recently, Shanmugharaj et al. [11] verified that, using high surface energy solvents, the interaction between aminosilanes and the edges of the clay platelets is reduced due to low wetting phenomena and, hence, the silane molecules can diffuse and react more efficiently in the mineral galleries.

The resulting Na-MMT dispersion and aminosilane solutions were then mixed, and the grafting reactions were carried out at 80 or 130 °C, under constant stirring for 3 h under nitrogen. After cooling, the reaction product was recovered by centrifugation at 13,000 rpm, and stabilized at 100 °C for 5 h in *vacuum* condition. Excess glycerol was removed by washing each reaction product with water under stirring at 60 °C for 1.5 h followed by centrifugation. This washing procedure was repeated three times, and the quantitative elimination of the solvent was confirmed by thermogravimetric analysis. Each resultant product was dried at 80 °C under *vacuum* and then ground to a powder. Procedure 1 was performed on all three aminosilanes, whereas Procedure 2 was carried out only in the case of A1100. In order to study the effect of the two silylation conditions on the final products, the interlayer spacings of the A1100-modified Na-MMTs obtained from the two procedures, were compared.

In order to determine the degradation temperatures of the silylated Na-MMT, two pastes with water and glycerol as dispersing agents were prepared to be tested by thermogravimetric analysis. In details, the Na-MMT/water paste (Na-MMT–H_2O) was obtained by dispersing Na-MMT powder in glycerol at 60 °C and then following the same procedure illustrated previously for the silylation reaction but without the addition of the aminosilane. The paste with glycerol (Na-MMT–Gly) was prepared by dispersing Na-MMT in glycerol at 60 °C. After centrifugation, the paste was kept in the oven for 22 h at 60 °C in *vacuum* condition.

2.3. Instrumental analyses

2.3.1. Fourier transform infrared analysis

Fourier transform infrared (FT-IR) spectra were performed by using a Nicolet FT-IR Fourier transform infrared spectrometer on KBr pressed disks containing 1% w/w of inorganic samples. FT-IR spectra were collected over the range 400–4000 cm^{-1} with a resolution of 4 cm^{-1}.

2.3.2. Thermogravimetric analysis

Thermogravimetric analysis (TGA) was carrying out on a TGA 2950 thermobalance (TA Instruments). Samples were heated from

Table 1
Reaction conditions adopted during the silylation process.

Procedure	Amount of Na-MMT in 100 ml of glycerol (g)	Amount of aminosilane in 100 ml of glycerol (g)	Reaction temperature (°C)
1	1	1	80
2	5	20	130

30 to 750 °C at a heating rate of 10 °C/min under nitrogen flow. The amount of grafted and intercalated aminosilanes was calculated using the following relationship [6]:

$$\text{Silane grafted amount (mequiv/g)} = \frac{10^3 \times W_{200-600}}{[100 - (W_{200-600})] \times M} \quad (1)$$

where $W_{200-600}$ corresponds to the mass loss between 200° and 600 °C and M (g/mol) is the molecular weight of the grafted silane molecules. The percentage of grafted amount, which corresponds to the percentage of organic aminosilane moieties with respect the total inorganic mass, was calculated as follows:

$$\text{Silane grafted amount (\%)} = \frac{100 \times W_{200-600}}{100 - W_{200-600}} \quad (2)$$

2.3.3. Wide angle X-ray diffraction analysis

The intergallery space between the clay platelets is defined as the basal spacing, and is usually denoted as d_{001} since it is derived from the (0 0 1) diffraction peak by using Bragg equation. The displacement of the (0 0 1) diffraction peak upon silylation was followed by WAXD measurements. To this end, an Anton Paar SAXSess diffractomer operating at 40 kV, 50 mA and equipped with a Cu Kα radiation (λ = 0.1542 nm) source and an image plate detector was used. The spectra were collected in the transmission mode. The scattering data were dark current and background subtracted, and normalized for the primary beam intensity.

2.3.4. Molecular dynamics analysis

All molecular dynamics (MD) simulations were performed using *Materials Studio* (v.4.4, Accelrys, San Diego, USA). The starting structure of Na-MMT was taken from previous work [15–19]. The main object of the computational part of this study was the prediction of the basal spacing in the aminosilane functionalized MMT. Since the quantities affecting the MMT basal spacing are highly sensitive to the non-bonded components of the force field (FF) employed (e.g., atomic charges and van der Waals parameters), the *ad hoc* FF developed by Heinz and coworkers [20,21] was adopted for the optimization of the initial MMT structure and in all subsequent calculations. As demonstrated by Heinz et al. [20,21] for Na-MMT and other phyllosilicates, this accurately derived FF is able to describe, among many other properties, the thermodynamics of surface processes more reliably by reducing deviations of 50–500% in surface and interface energies to less that 10%, thus constituting a fundamental step towards a quantitative modeling of interface processes involving layered silicates.

Accordingly, the resulting lattice of the optimized MMT model was monoclinic, with space group C2/m, and characterized by the following lattice parameters: a = 5.20 Å, b = 9.20 Å, c = 10.13 Å, and $\alpha = 90°$, $\beta = 99°$, $\gamma = 90°$, in excellent agreement with the available literature [21–24].

According to the computational recipe adopted, the molecular models of the aminosilane compounds considered (see Scheme 1) were built and geometry-optimized following a well-validated MD-based protocol [15–19,32].

The optimized MMT unit cell model was then modified by grafting the layers with a suitable number of aminosilane molecules [15]. For each aminosilane, three possible options were considered for creating covalent bonds between the silicon (Si) atoms of the aminosilane and the MMT surface oxygen (O) atoms, as illustrated in Scheme 2.

The new equilibrium position of the Na^+ counterions on the aminosilane-modified MMT sheets were determined following the procedure suggested by Heinz et al. [21]. Accordingly, half of them were placed 1 nm away on one side, and the remaining half 1 nm from the other side of the MMT layer in 10 different arrangements. Molecular mechanics energy minimizations were then performed to convergence, keeping all other MMT atoms fixed, and the structure with the lowest energy was finally selected for further simulations. In this configuration, the Na^+ ions were found at about 1.8 Å from the center of the surface oxygen atoms, or

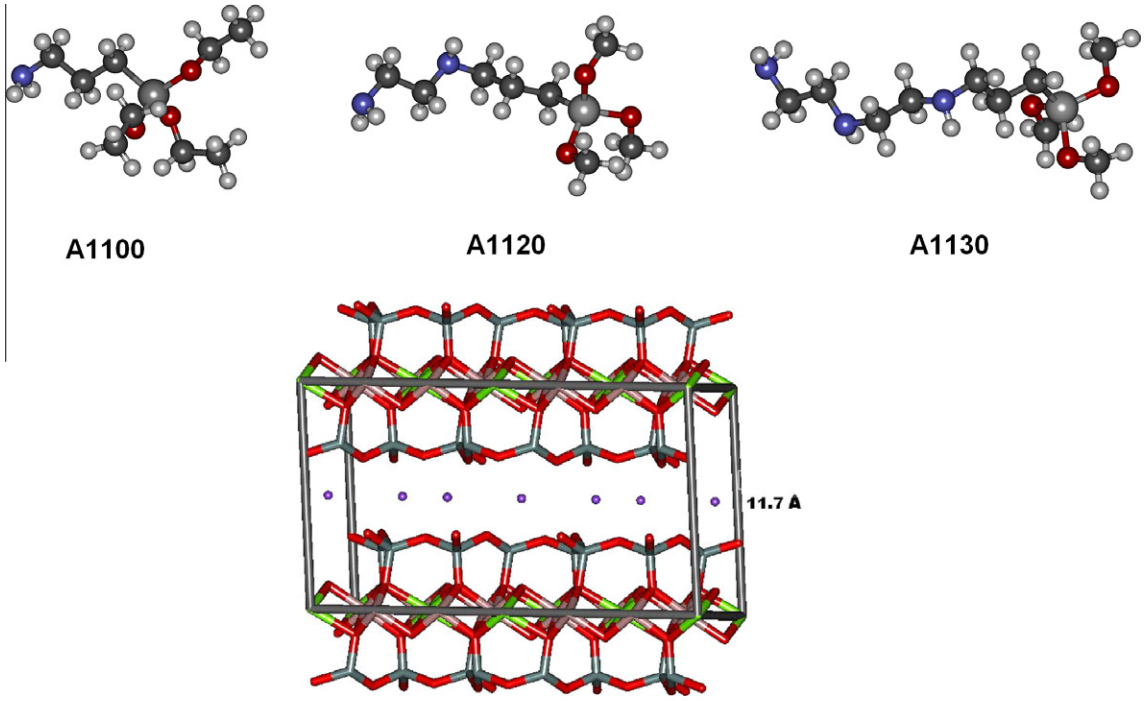

Scheme 1. Chemical structures of the considered aminosilanes and crystallographic unit cell of MMT. The atom color code is as follows: gray, C; light gray, Si; blue, N; red, O, white, H; purple, Na; green, Al; pink, Mg. (For interpretation of the references to color in this figure legend, the reader is referred to the web version of this article.)

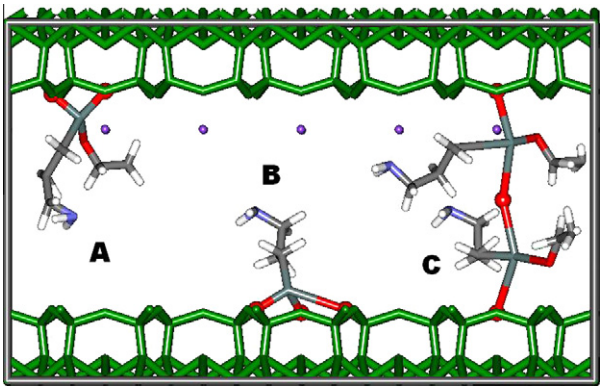

Scheme 2. Schematic representation of possible covalent bonds formation between the Si atoms of the aminosilane molecules and the MMT surface O atoms. A: two covalent bonds on the same MMT surface; B: three covalent bonds on the same MMT surface; C: two covalent bonds bridging two MMT layers.

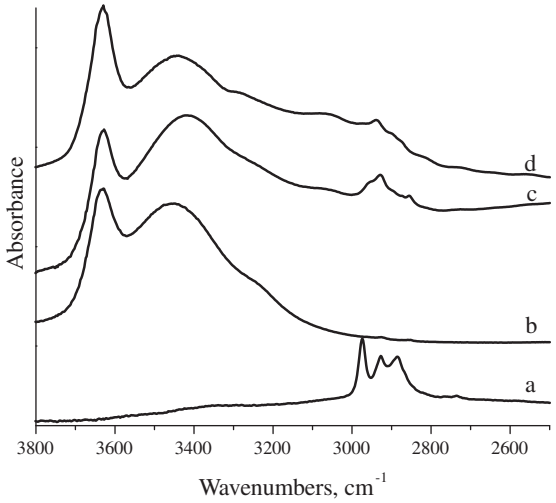

Fig. 1. Infrared spectra of: (a) A1100; (b) pristine Na-MMT; (c) A1100-MMT obtained from Procedure 1; (d) A1100-MMT obtained from Procedure 2.

about 4.8 Å from the central plane of the metal atoms, in excellent agreement with previous simulations [33] and experimental NMR data [34].

Lastly, each aminosilane-MMT unit cell was replicated four times in the *a* direction, and three times in the *b* direction, thus yielding a final simulation supercell for each aminosilane modifier with the following lattice parameters: $a = 20.80$ Å, $b = 27.60$ Å, and $\alpha = 90°$, $\beta = 99°$, $\gamma = 90°$. The *c* values in the initial model of aminosilane-MMT supercells were prolonged according to a bi-layer arrangement of each aminosilane molecules.

Molecular mechanics (MM) and molecular dynamics (MD) simulation protocols were then applied, consisting of a preliminary cell energy minimization procedure followed by isobaric-isothermal (NPT) MD runs at 300 K. To avoid crystal structure deformation during minimization, initially both MMT layers were treated as rigid bodies by fixing all cell dimensions except the *c* axis, whilst all atoms in the interlayer space including the cations were allowed to move without any constraint. Then, in a second minimization round, also movement along the *c* axis was allowed, leading to a suitable starting interlayer distance for each model. Subsequently, 1 ns NPT MD experiments were performed at 300 K for each system, using the Verlet algorithm and an integration step of 1 fs. Again, both MMT layers were treated as rigid bodies by fixing all cell dimensions except the *c* axis, leaving all remaining atoms in the interlayer space free to move without any constraint. The Ewald summation method [35] was applied for treating both van der Waals and electrostatic interactions, while temperature was controlled using the Nosé thermostat [36].

The final basal spacing values for each aminosilane-MMT system were extracted from the final part (0.5 ns) of the equilibrated MD trajectory.

3. Results and discussion

3.1. Fourier transform infrared analysis

Infrared spectroscopy was performed in order to verify the silylation process and to identify the presence of the organic moieties on the Na-MMT platelets due to silylation. As pointed out by Zhao et al. [13], the main evidence for the successful intercalation/silylation of the aminoalkylsilanes in the Na-MMT galleries is the presence of C–H and N–H absorbance peaks in the corresponding IR spectra. Fig. 1 shows an enlargement of the IR between 3800 and 2500 cm^{-1} for the A1100-MMT sample using the two different procedures described above. In the same figure, the spectra of the A1100 silane molecule and the pristine Na-MMT are also shown for comparison.

Compared to the neat Na-MMT spectrum, the two functionalized powders show additional peaks which can be attributed to the asymmetric and symmetric stretching vibrations of the methylene groups at 2936 and 2885 cm^{-1}, respectively, thus confirming the presence of the organic moieties on the Na-MMT surface [25–27]. A shoulder at ~3290 cm^{-1} in Fig. 1 may be assigned to the stretching of the NH_2 group [28]. It is worth noting that, by increasing the aminosilane concentration and the reaction temperature, both methylene and NH_2 adsorption peaks in Fig. 1 become progressively more pronounced, suggesting the presence of a larger amount of intercalated/grafted silane modifiers. No evaluation was performed on the relative intensity of the peaks related to the stretching vibration of isolated or hydrogen bonded OH groups (at 3620 cm^{-1} and 3440 cm^{-1}, respectively), because the possible presence of adsorbed water cannot be ruled out [29].

3.2. Thermogravimetric analysis

Thermogravimetric analysis (data not shown) was carried out on the Na-MMT powders prior and after the silylation reaction performed by Procedure 1. The mass losses in the range between 200° and 600 °C were used as entry parameters in Eqs. (1) and (2) to evaluate the grafted aminosilane amounts, and the corresponding results are displayed in Table 2. Interestingly, by the application of Procedure 1 the grafted aminosilane amounts increase with increasing of the aminosilane alkyl chain.

Table 2
Thermogravimetric analysis of functionalized MMT.

		Mass loss[a] (%)	Grafted amount[b] (mequiv/g)	Grafting amount[c] (%)
A1100-MMT	Procedure 1	8.8	0.4 (I = 68%; S = 32%)	9.6
	Procedure 2	11.4	0.6 (O = 21%; I = 38%; S = 41%)	12.8
A1120-MMT		14.6	0.8	17.1
A1130-MMT		18.8	0.9	23.2

[a] Mass loss between 200° and 600 °C.
[b] Determined by using Eq. (1).
[c] Determined by using Eq. (2).

In order to identify the degraded species, two pastes obtained by dispersing the Na-MMT in water and glycerol, respectively, were analyzed. The results are displayed in terms of first derivative mass loss in Fig. 2.

The pristine Na-MMT shows two Fig. 2 peaks at 50 and 630 °C corresponding to the physically adsorbed water and the dehydroxylation of the clay, respectively [30,31]. The curve related to the Na-MMT–H_2O paste shows a peak at 50 °C related to the loss of physically adsorbed water, whereas the two other peaks at 270 and 358 °C (Fig. 2) can be sensibly ascribed to the loss of intercalated water. By analogy, the intense Fig. 2 peak at 215 °C in the Na-MMT–Gly curve could be assigned to the loss of physically adsorbed glycerol, whilst the weak Fig. 2 peak at ~350 °C could refer to the intercalated glycerol. As for the Na-MMT–H_2O paste, the Fig. 2 peak at higher temperature is due to MMT dehydroxylation. The DTG curves of the A1100-MMT system shows the mass loss of physically adsorbed water at 50 °C, and other two Fig. 2 peaks at 418 and 540 °C, respectively. The first one is ascribable to the intercalated aminosilanes, whereas the broad Fig. 2 peak at 540 °C could be linked to the decomposition of the chemically bound aminosilanes [9]. Due to the consumption of hydroxyl groups belonging to the platelet edges, the Na-MMT dehydroxylation Fig. 2 peak at 630 °C nearly vanishes for this system. Lastly, the absence of the Fig. 2 peak at 215 °C related to the physically adsorbed glycerol speaks in favor of the reliability of the applied washing procedure.

With the goal of evaluating the effect of the reaction parameters (i.e. temperature and aminosilane concentration) on the silylation process, the amount of intercalated and grafted aminosilane was assessed by performing TGA analysis on the A1100-MMT systems obtained by using the two different reaction routes summarized in Table 1. To eliminate the different contributes due to dissimilar adsorbed amounts of water, the curves shown in Fig. 3 A were normalized assigning to each curve the value of 100 to the mass achieved at 150 °C. It is worth noting that, as we will discuss later, by increasing both temperature and aminosilane concentration, the quantity of aminosilanes able to penetrate into the Na-MMT gallery platelets slightly increases. Moreover, the grafted aminosilane amount increased by using the Procedure 2 compared to Procedure 1 (see Table 2). The DTG analysis performed on the A1100-MMT product obtained by Procedure 1 (Fig. 3 B)) shows the presence of two peaks at 418 and 540 °C, ascribed to the intercalated aminosilanes and chemically bounded aminosilanes, respectively [9].

Interestingly, the A1100-MMT product prepared following Procedure 2 displays a third Fig. 3B peak at 310 °C, which could be attributed to the aminosilane interacting with the outer surfaces of the clay platelets.

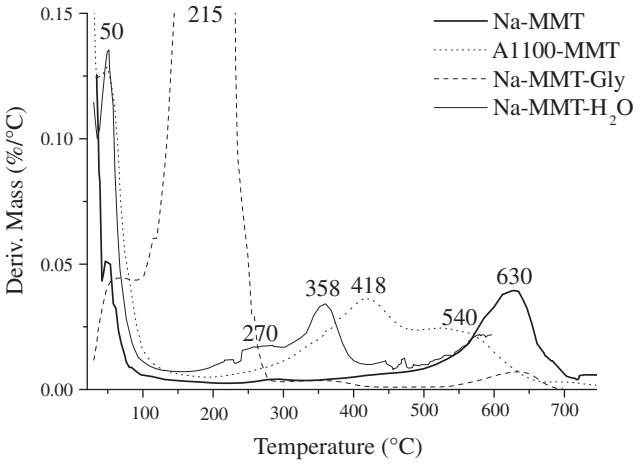

Fig. 2. DTG curves of pristine Na-MMT, functionalized Na-MMT powders, and Na-MMT/water and Na-MMT/glycerol pastes.

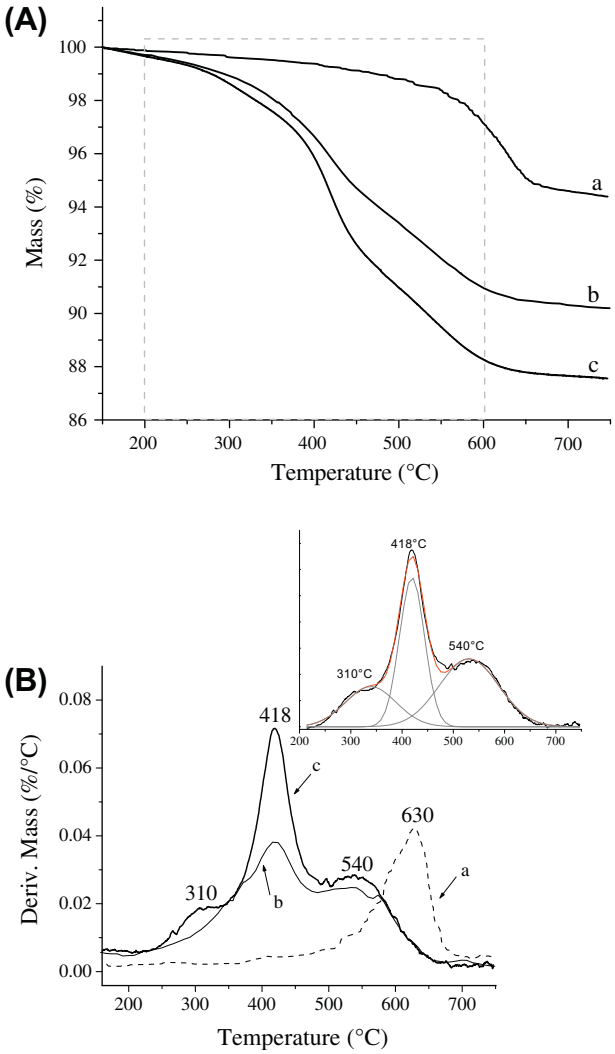

Fig. 3. Thermogravimetric analysis of Na-MMT before and after silylation reaction using two different process parameters: (A) mass losses curve; (B) first derivative of mass losses curve. The inset shows the peak deconvolutions: (a) pristine Na-MMT; (b) A1100-MMT obtained from Procedure 1; (c) A1100-MMT obtained from Procedure 2.

With these peaks assignments in mind, it was possible to quantify each degraded moieties using the deconvolution method of the Origin program. The results of these deconvolutions are summarized in Table 2, where *O* indicates the aminosilane interacting with the outside platelets, and *I* and *S* are the intercalated and chemically bonded aminosilanes, respectively. The results show that higher temperature and aminosilane concentration values lead to an increased amount of chemically bonded silanes with respect to the intercalated species. Moreover, and perhaps more interestingly, only the A1100-MMT obtained by Procedure 2 displays aminosilanes interacting with the outside platelets.

3.3. Wide angle X-ray diffraction results and molecular dynamics predictions

To quantify the effect of the length of the aminosilane alkyl substituents on the Na-MMT basal spacing, silylation reactions were performed using the three different aminosilanes A1100, A1120 and A1130, and adopting Procedure 1. The X-ray diffraction

patterns related to the (0 0 1) basal spacing, displayed in Fig. 4, show that the introduction of any aminosilane type into the Na-MMT gallery shifts the peak at lower 2θ values compared to the pristine Na-MMT.

This increase of basal spacing is a clear signal that each aminosilane species has been grafted/intercalated in the inter-platelets space of Na-MMT. In detail, the neat Na-MMT shows a Fig. 4 peak at 2θ equal to 7.5°, corresponding to a *d*-spacing value of 11.7 Å, whereas the aminosilane-modified MMTs show Fig. 4 diffraction peaks at 2θ values between 5.3° and 5.9° (Table 3). Concerning the effect of the alkyl chain length, the A1120-MMT and A1130-MMT systems show lower basal spacing values, 15.3 and 15.0 Å, respectively, compared to the A1100-MMT, for which d_{001} = 16.7 Å. A major, important conclusion which can be drawn from the analysis of data shown in Table 3 is that the longer the organic chain on the aminosilane molecules, the smaller the *d*-spacing in the relevant modified MMT.

To try to find a molecular rationale for the somewhat counter-intuitive behavior reported above, molecular dynamics (MD) simulations have been performed on model systems.

Table 4 shows the values of estimated aminosilane-MMT interlayer spacing for all model systems considered (see Scheme 1) as obtained from 1 ns NPT MD simulations. From these values, and the inspection of the relevant MD trajectories, we can draw some useful considerations.

First of all, independently of the aminosilane chain length, aminosilane molecules bridging two MMT layers (i.e., option C in Scheme 2) result in the lowest *d*-spacing values (see Table 4). From the viewpoint of further employment of aminosilane-MMT systems for polymer intercalation and/or exfoliation, this is the worst case possible, as the distance between MMT sheets is not only practically coincident with that of unmodified MMT (i.e., 11.7 Å), but also the aminosilane molecules act as 'anchoring points", counteracting any eventual macromolecular intercalation/exfoliation. Fig. 5 shows an equilibrated MD snapshot of the A1100-MMT/option C system as an example.

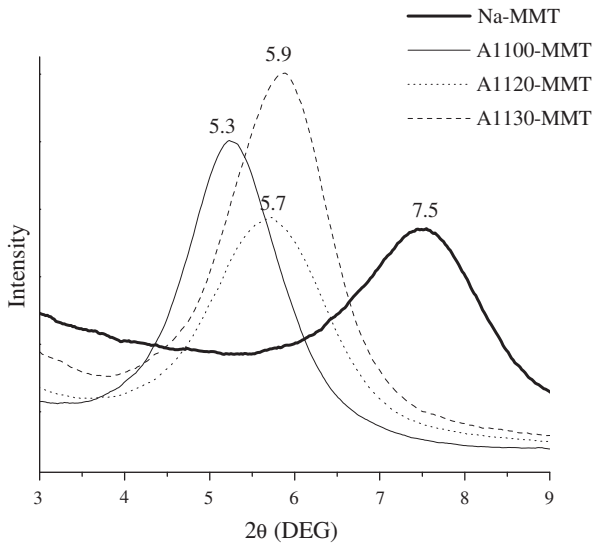

Fig. 4. X-ray diffraction patterns of Na-MMT before and after silylation reaction with different aminosilanes.

Table 3
d-Spacing values for aminosilane-modified MMT estimated by XRD analysis.

System		2θ (°)	*d*-Spacing (Å)
Pristine Na-MMT	Procedure 1	7.5	11.7
A1100-MMT	Procedure 2	5.3	16.7
		4.0	22.2
A1120-MMT		5.7	15.3
A1130-MMT		5.9	15.0

Table 4
d-Spacing values for aminosilane-modified MMT estimated by MD simulations.

System	*d*-Spacing (Å)			
	Option A[a]	Option B[a]	Average A and B	Option C[a]
A1100-MMT Procedure 1	17.0	16.2	16.6	11.7
A1100-MMT Procedure 2	21.9	21.7	21.8	11.7
A1120-MMT	15.9	15.3	15.6	11.9
A1130-MMT	15.1	14.8	14.9	11.9

[a] For the meaning of Options A–C, please refer to Scheme 2.

The results obtained for the two alternative bonding options (i.e., A and B in Scheme 2), expressed as average *d*-spacing values (see 3rd column in Table 4), are in excellent agreement with the experimental evidences discussed above. Notably, however, in contrast to common observations during the intercalation of small molecules between the silicate layers, where longer organic chains normally result in higher interlayer spacing, for aminosilane-MMT systems a reverse trend is observed. Indeed, longer aminosilane molecules yield lower *d*-spacing.

A sensible explanation for this coupled experimental/simulation evidence could be hypothesized, keeping in mind that the organic tail of each aminosilane molecule features not only $-CH_2$ groups, which are hydrophobic, but also one or more $-NH_2$/NH– groups, which are endowed with hydrophilic character, and capable to originate both intra- and inter-molecular hydrogen bonds (see Scheme 1).

Following these lines of reasoning, for the smaller aminosilane molecule A1100, characterized by the presence of a short chain and only one terminal $-NH_2$ group, a mechanism quite similar to that observed for quaternary ammonium salt-modified MMT can be envisaged. Accordingly, the A1100 aminosilane chains are attracted by the surface of clay and, while flattening onto it, provide a screening between the charges of the MMT layers ultimately favoring the weakening of interlayer attraction and, hence, a larger *d*-spacing value.

On the other hand, the other two aminosilane molecules (A1120 and A1130), featuring longer, more mobile chains with one and two –NH groups, respectively, have a strong tendency to interact among themselves (*via* both intermolecular hydrogen bonding and hydrophobic interactions). As a result, their flattening onto the MMT surface is reduced, the charge distribution on the MMT

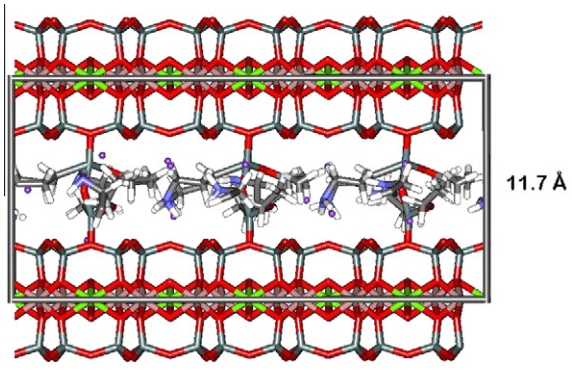

Fig. 5. Equilibrated MD snapshot of the A1100-MMT/option C system (see Scheme 2).

surface is less screened, and the clay sheets do not tend to separate as much as in the case of A1100 chains. Fig. 6a and b show a comparison between two equilibrated MD snapshots for A1100-MMT and A1120-MMT, respectively, in which the different degree of interactions between the aminosilane chains, resulting in a smaller *d*-spacing, is well evident.

The A1100-MMT system was further selected to check the effect of the preparation procedure adopted. Fig. 7 shows the diffraction patterns related to the A1100-MMT obtained by using the two procedures summarized in Table 1.

For the sake of comparison, the diffraction pattern of the pristine Na-MMT is also reported. In details, the silylation reaction with A1100 by Procedure 2 resulted in a further shift of the (0 0 1) diffraction peak up to $2\theta = 4.0°$, corresponding to a *d*-spacing value of 22.2 Å, with respect to that obtained with the silylation by Procedure 1 (16.7 Å). It is worth noting that the highest reaction temperature and aminosilane concentration (i.e. Procedure 2) allowed obtaining a higher enlargement of the basal spacing. Moreover, the broader Fig. 7 (0 0 1) diffraction peak reflects the variety of platelets gallery heights due to the grafted/intercalated products.

In harmony with the experimental findings, the MD simulations reveal that, upon increasing the number of aminosilane molecules within the clay galleries indeed results in a larger value of the estimated *d*-spacing, which, in turn, is in excellent agreement with the corresponding experimental evidence (see values in Tables 2 and 3). Fig. 6c yields pictorial evidence in support to the numerical value. As can be easily seen by comparing Fig. 6a and c, when more aminosilane molecules are grafted/intercalated into the clay galleries the surface of the MMT layers is better screened by the silane hydrocarbon chains. Accordingly, the attraction forces among the layers are weakened, and the resultant distance between them is higher. Not only, but, in the presence of higher silane concentration, the hydrocarbon chains of neighboring molecules grafted/physical bounded to the same clay layer tend to interact more among themselves than with those laying on the opposite sheet. And this factor further concurs to lessen the overall attraction between facing sheets and, hence, a higher d_{001} value.

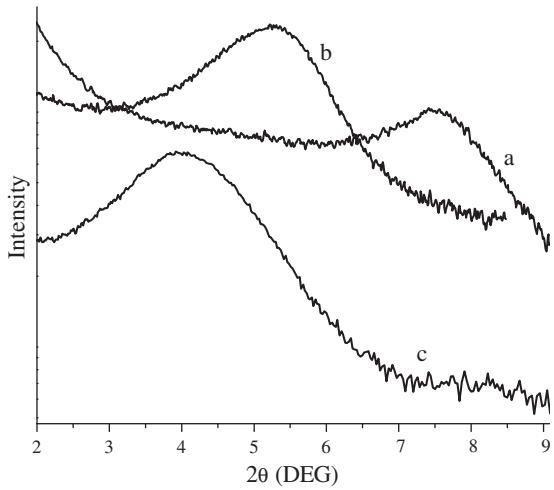

Fig. 7. XRD analyses performed on the Na-MMT before and after silylation reaction carried out using two different process conditions. (a) pristine Na-MMT; (b) A1100-MMT obtained with Procedure 1; (c) A1100-MMT obtained with Procedure 2.

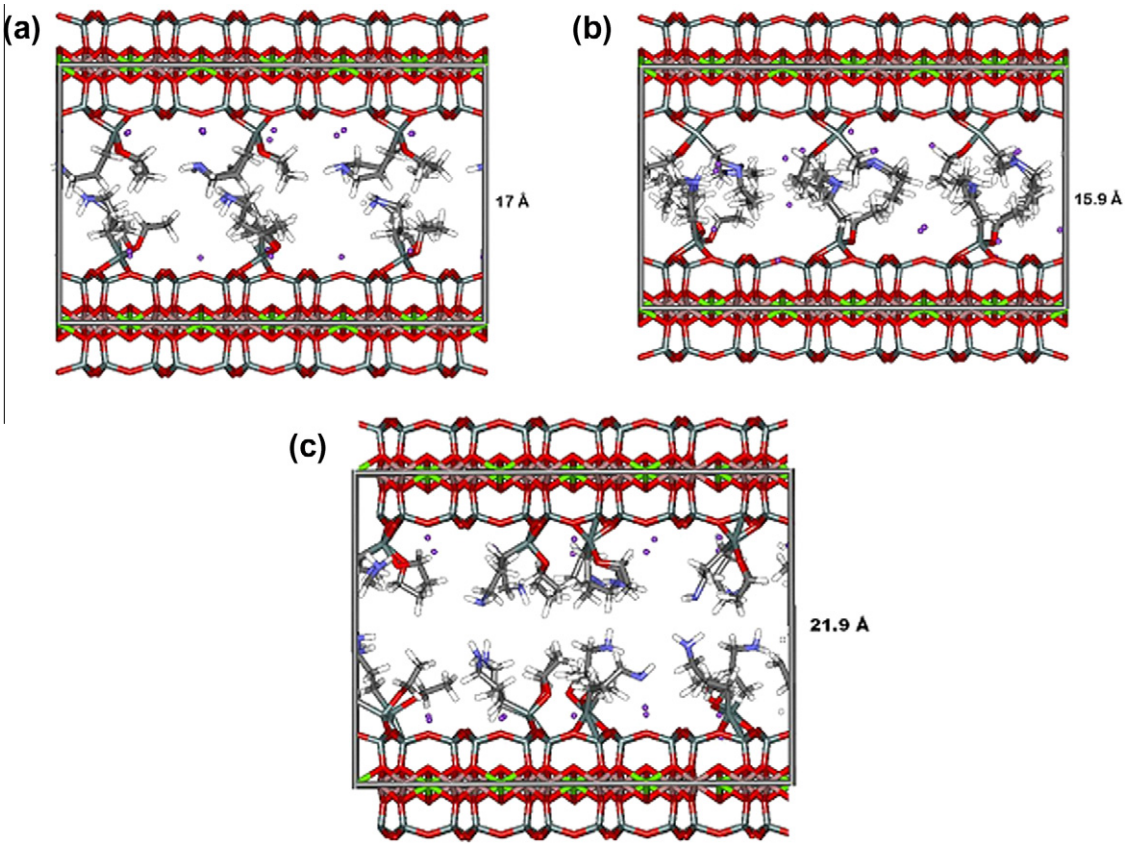

Fig. 6. Equilibrated MD snapshot of (a) A1100-MMT/option A, reaction Procedure 1, (b) A1120-MMT/option A, and (c) A1100-MMT/option A, reaction Procedure 2 systems (see Scheme 2).

4. Conclusions

Three aminosilanes (A1100, A1120 and A1130) characterized by different lengths of the alkyl chains are used to functionalize the Na-MMT, by following two different routes in terms of reaction temperature and aminosilane concentration. The appearance in the FT-IR spectra of additional peaks at 2936 and 2885 cm^{-1}, attributed to the asymmetric and symmetric stretching vibrations of the methylene groups, respectively, and a shoulder at $\sim$3290 cm^{-1} assigned to the stretching of the NH_2 group, confirm the presence of the organic moieties on the Na-MMT surface. The thermogravimetric analyses show that higher temperature and aminosilane concentration values lead to aminosilanes interacting with the outside platelets and an increased amount of chemically bonded silanes with respect to the intercalated species. The WAXD analyses show that the introduction of any aminosilane type into the Na-MMT gallery allows the basal spacing to increase with respect to the pristine Na-MMT, which is a clear signal that each aminosilane species has been grafted/intercalated in the inter-platelets space. Moreover, the WAXD analyses highlight the surprising result that the longer the organic chain on the aminosilane molecules, the smaller the *d*-spacing in the relevant modified MMT. The molecular dynamics simulation explains this result in light of the strong tendency of A1120 and A1130 aminosilanes to interact among themselves by both intermolecular hydrogen bonding and hydrophobic interactions because of the presence of one or two –NH groups in their organic chains. On the other hand the A1100 molecules, owing only one $–NH_2$ group, provide a better screening between the MMT layers ultimately favoring the weakening of interlayer attraction and, hence, a larger *d*-spacing value.

Acknowledgments

The authors thank IMAST and MIUR. This work was supported by the research project MACE coded MIUR n. DM24442.

References

[1] J. Zhang, R.K. Gupta, C.A. Wilkie, Polymer 47 (2006) 4537.
[2] H. Shi, T. Lan, T.J. Pinnavaia, Chem. Mater. 8 (1996) 1584.
[3] S. Yariv, H. Cross, in: Dekker M, (Eds.), Clays and Clay Minerals, New York, 2002. pp. 463–566.
[4] L.A. Utracki, Clay-containing Polymeric Nanocomposites, Rapra Technology Limited Press, Shrewsbury, 2004.
[5] P.A. Wheeler, J. Wang, J. Baker, L.J. Mathias, Chem. Mater. 17 (2005) 3012.
[6] N.N. Herrera, J.M. Letoffe, J.L. Putaux, L. David, E. Bourgeat-Lami, Langmuir 20 (2004) 1564.
[7] A.Y. Park, H. Kwon, A.J. Woo, S.J. Kim, Adv. Mater. 17 (2005) 106.
[8] N. Herrera, J. Letoffe, J. Reymondc, E. Bourgeat-Lami, J. Mater. Chem. 15 (2005) 863.
[9] H. He, J. Duchet, J. Galy, J. Gerard, Colloid. Interface Sci. 288 (2005) 171.
[10] M. Park, I.K. Shim, E.Y. Jung, J.H. Choy, J. Phys. Chem. Solids 65 (2004) 499.
[11] A.M. Shanmugharaj, K.Y. Rhee, S.H. Ryu, J. Colloid Interface Sci. 298 (2006) 854.
[12] A. Di Gianni, E. Amerio, O. Monticelli, R. Bongiovanni, Appl. Clay Sci. 42 (2008) 116.
[13] C. Zhao, M. Feng, F. Gong, H. Qin, M. Yang, J. Appl. Polym. Sci. 93 (2004) 676.
[14] K. Wang, L. Wang, J. Wu, L. Chen, C. He, Langmuir 21 (2005) 3613.
[15] M. Fermeglia, M. Ferrone, S. Pricl, Fluid Phase Equilib. 212 (2003) 315.
[16] R. Toth, A. Coslanich, M. Ferrone, M. Fermeglia, S. Pricl, S. Miertus, E. Chiellini, Polymer 45 (2004) 8075.
[17] G. Scocchi, P. Posocco, A. Danani, S. Pricl, M. Fermeglia, Fluid Phase Equilib. 261 (2007) 366.
[18] M. Fermeglia, M. Ferrone, S. Pricl, Mol. Simul. 30 (2004) 289.
[19] G. Scocchi, P. Posocco, J.W. Handgraaf, J.G.E.M. Fraaije, M. Fermeglia, S. Pricl, Chem. Eur. J. 15 (2009) 7586.
[20] H. Heinz, U.W. Suter, J. Phys. Chem. B 108 (2004) 18341.
[21] H. Heinz, H. Koerner, K.L. Anderson, R.A. Vaia, B.L. Farmer, Chem. Mater. 17 (2005) 5658.
[22] G. Brown, The X-ray Identification and Crystal Structures of Clay Minerals, Mineralogical Society Press, London, 1961.
[23] S.W. Bayley, Reviews in Mineralogy, Mineralogical Society of America Press, Chelsea, Michigan, 1988. <http://www.webmineral.com>.
[24] S.I. Tsipurski, V.A. Drits, Clay Miner. 19 (1984) 177.
[25] K. Endo, Y. Sugahara, K. Kuroda, Bull. Chem. Soc. Jpn. 67 (1994) 3352.
[26] T. Yankgisawa, K. Kurodo, C. Kato, React. Solids 5 (1988) 167.
[27] S. Okutomo, K. Kuroda, M. Ogawa, Appl. Clay Sci. 15 (1999) 253.
[28] I.K. Tonle, E. Ngameni, D. Njopwouo, C. Carteret, A. Walcarius, Phys. Chem. Chem. Phys. 5 (2003) 4951.
[29] E. Ruiz-Hitzky, J.M. Rojo, G. Lagaly, Colloid. Polym. Sci. 263 (1985) 1025.
[30] C. Wan, X. Bao, F. Zhao, B. Kandasubramanian, M.P. Duggan, J. Appl. Polym. Sci. 110 (2008) 550.
[31] S. Yariv, Appl. Clay Sci. 24 (2004) 225.
[32] R. Toth, D.J. Voorn, J.W. Handgraaf, J.G.E.M. Fraaije, M. Fermeglia, S. Pricl, P. Posocco, Macromolecules 42 (2009) 8260.
[33] E. Hackett, E. Manias, E.P. Giannelis, Chem. Mater. 12 (2000) 2161.
[34] D.K. Yang, D.B. Zax, J. Chem. Phys. 110 (1999) 5325.
[35] P.P. Ewald, Ann. Phys. 64 (1921) 253.
[36] S. Nosé, Prog. Theor. Phys. Suppl. 103 (1991) 1–46.